MICHIGAN STATE UNIVERSITY

CYCLOTRON LABORATORY

MEAN FIELD DYNAMICS AND NON-EQUILIBRIUM PARTICLE EMISSION

M.B. TSANG

Invited talk to be published in the Proceedings of the Symposium on Central Collisions and Fragmentation Processes, Denver, Co, U.S.A., April 1987

MAY 1987

MSUCL-606

MSUCL-606
May 1987

MEAN FIELD DYNAMICS AND NON-EQUILIBRIUM PARTICLE EMISSION

M.B. Tsang

National Superconducting Cyclotron Laboratory,
Michigan State University, E. Lansing, MI 48824, U.S.A.

A strong preference for the emission of nonequilibrium light particles in the reaction plane was observed, suggesting the existence of collective motion of the emitting source for intermediate energy heavy ion reactions. The sign of the average emission angle of non-equilibrium charged particles ($1 \leq Z \leq 15$) was determined for ^{14}N-induced reactions on ^{154}Sm at E/A=35 MeV from the circular polarization of coincident γ-rays emitted from the residual nucleus. All the detected charged particles are preferentially emitted to negative angles. These effects are consistent with deflection of the particles to the reaction plane and to negative scattering angles by the attractive nuclear mean field. Numerical solutions of the Boltzmann-Uehling-Uhlenbeck equation demonstrate that the experimental result is sensitive to the interplay between nuclear mean field and nucleon-nucleon collisions. By extending the calculations to higher energies, the sign of the emission angles is predicted to change above E/A = 100 MeV.

1. INTRODUCTION

The dynamics of intermediate energy nucleus-nucleus reactions are governed by the nuclear mean field and by collisions between individual nucleons. Each effect evolves dramatically as the bombarding energy is increased. At low energies (E/A≤10 MeV), the mean field is predominantly attractive and individual nucleon-nucleon collisions are hindered by the Pauli exclusion principle. At much higher energies (E/A≥100 MeV), nucleon-nucleon collisions are frequent and densities may be achieved where the nuclear mean field becomes repulsive.[1,2] The transition from mean field dominated dynamics of low energy reactions to nucleon-nucleon collision dominated dynamics of high energy reactions is expected to occur at incident velocities comparable to the Fermi velocity where Pauli-blocking becomes less effective. In addition, the transition between deeply inelastic processes to fragmentation processes is expected to occur in this energy domain.[3]

2. ENHANCED EMISSION OF NONEQUILIBRIUM LIGHT PARTICLES IN THE REACTION PLANE

One of the signatures for the importance of mean field effects in intermediate heavy ion reaction is the observation of collective motion by the participating nucleons. This is manifested by the preferential emission of nonequilibrium light particles (p, d, t, α) to the entrance channel reaction plane.[4,5]

2.1. Experiment

A ^{197}Au target of 0.5 mg/cm² areal density was bombarded with ^{14}N ions of 420 MeV incident energy. Coincident fission fragments were detected with two position-sensitive parallel-plate detectors θ_x = 70°, ϕ_x= 0° and θ_x = 80°, ϕ_x= 180°, respectively. Since the angular momentum of the fissioning system is nearly perpendicular to the entrance channel reaction plane, we define the reaction plane as the plane containing the coincident fission fragments and the beam axis. Two light particle telescopes consisting of Si ΔE and NaI E detectors were placed at angles θ_x = 55°, ϕ_x= 0° (in the reaction plane) and θ_x = 55°, ϕ_x= 90° (out of the reaction plane).

2.2. Experimental Results

The energy spectra of light particles detected in and out of plane with two coincident fission fragments are shown by circular and triangular points in Fig. 1. Similar to previous observations for slightly different systems, the energy spectra exhibit approximately Maxwellian shapes. However, there is a clear preference for the emission of energetic light particles in the plane of the outgoing fission fragments. To provide a quantitative measure of this enhancement, the ratios of out-of-plane to in-plane coincidence cross-sections have been plotted in Fig. 2 as a function of the energy of the emitted particles. The horizontal bars in the figure show the energy intervals over which the coincidence cross sections were integrated. The ratios decrease significantly with increasing energy and with increasing mass of the coincident light particles. For high energy alpha particles, azimuthal anisotropies of up to one order of magnitude are observed. Similar azimuthal anisotropies have also been observed for the emission of intermediate mass fragments in the ^{32}S induced reactions on Ag at E/A = 22.5 MeV.[6]

2.3. Model Calculations

The observed enhanced emission of nonequilibrium particles in the reaction plane can be understood by assuming the existence of an

ordered collective motion of the emitting source in the reaction plane and transverse to the beam.

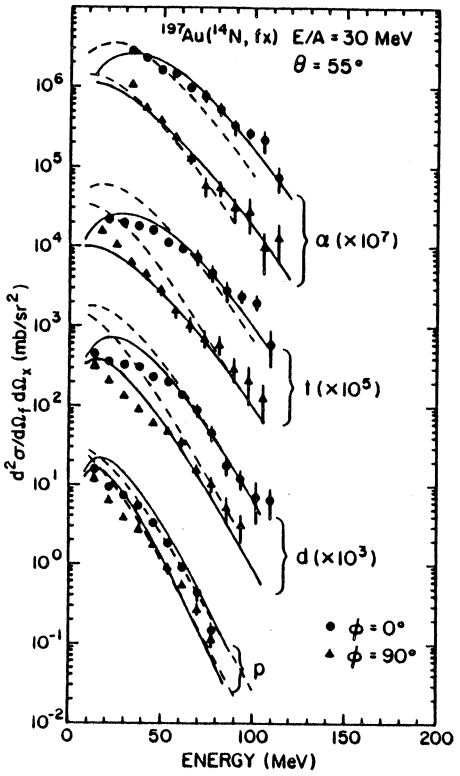

FIGURE 1
Energy Spectra of p, d, t and α particles measured in coincidence with fission fragments for ^{14}N induced reactions on ^{197}Au at E/A = 30 MeV. The solid and dashed curves are model calculations explained in text.

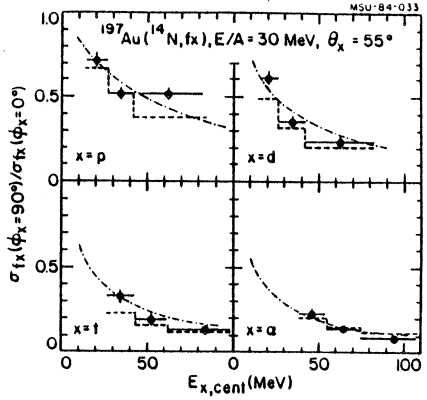

FIGURE 2
Ratios of out-of-plane to in-plane coincidence cross-sections as a function of the emitted particles energy. The dashed histograms and dot-dashed curves are model calculations.

For illustration, we performed two schematic calculations. In the first calculation we adopted a model of an emitting source which rotates with angular frequency ω about an axis perpendicular to the entrance channel scattering plane while moving with a velocity v_o parallel to the beam axis. In a semiclassical approximation the cross section in the laboratory frame may be expressed as

$$\frac{d^2\sigma_x}{dE_x\,d\Omega_x}(E_x,\theta_x,\Phi_x)=N\sqrt{(E_x E_{c.m.})}\exp\left[\frac{-E_{c.m.}}{T}\right]\frac{J_1(iA\sqrt{(E_{c.m.}-E_x\sin^2\theta_x\sin^2\Phi_x)})}{iA\sqrt{(E_{c.m.}-E_x\sin^2\theta_x\sin^2\Phi_x)}} \quad (1)$$

where N is a normalization constant; J_1 denotes the first-order Bessel function; $A = \sqrt{(2m)}R\omega/T$; $E_{c.m.} = E_x + E_o - 2\sqrt{(E_x E_o)}\cos\theta_x$; $E_o = 1/2mv_o^2$; E_x and m are the energy and mass of the emitted particle; θ_x and Φ_x are the polar and azimuthal angles of the emitted particle; and R and T are the radius and temperature of the source.

In the second calculation, we assumed that the ordered motion is purely translational with a significant velocity component perpendicular to the beam in the entrance-channel scattering plane. We use a moving source parametrization corresponding to a Maxwellian distribution in a rest frame which moves with the velocity v_o at the polar and azimuthal angles θ_o and $\Phi_o = 0$, respectively. In the laboratory frame, the differential cross section is given by

$$\frac{d^2\sigma_x}{dE_x\,d\Omega_x}(E_x,\theta_x,\Phi_x) =$$

$$N'\sqrt{E_x}\cdot\exp\left[\left[-E_x+E_o-2\sqrt{(E_x E_o)}(\cos\theta_x\cos\theta_o+\sin\theta_x\sin\theta_o\cos\Phi_x)\right]/T\right] \quad (2)$$

where N' is a normalization constant.

Details of these calculations are given in Ref. 4. The results are compared to the experimental measurements in Figs. 1 and 2. Calculations with the rotating source (equation 1) appear as solid lines in Fig. 1 and as dashed histograms in Fig. 2. The parameters used in these calculations are T=5.8 MeV, v_o=0.09c and Rω=0.1c for the emission of p, d and t and Rω = 0.08c for the emission of α particles. The dashed lines in Fig. 1 and the dot-dashed lines in Fig. 2 were calculated with the sideways moving source (equation 2) with parameters T=7 MeV, v_o=0.1c and θ_s = 29°. In both parametrizations the component of the source velocity parallel to the beam axis is assumed to be about 40% of the beam velocity. The large magnitude of the transverse collective velocities (Rω = 0.08c, $v_o\sin\theta_s$ = 0.05c) implies a collective velocity which is too fast to be consistent with a rigid rotation of the compound nucleus.

It should be noted that the temperature parameter T obtained by fitting the inclusive energy spectra with the rotating emitting

source is consistently lower than the temperature obtained when the rotation of the moving source is neglected.[4,7] Similar effects are reported by W. Friedman at this conference[8] for emission from an equilibrated rotating compound nucleus. If one increases the angular velocity of the source while holding the temperature fixed, the collective rotation tends to make the slopes of the energy spectra less steep. Consequently, increasing temperature and increasing angular velocity have similar effects on the energy spectra. If the collective motion, parametrized here by the angular velocity of the source, is not established without ambiguity, it is not possible to extract accurate temperatures from kinectic energy spectra.

Microscopically, the collective motion can be understood in terms of the macroscopic flow mediated by the mean field. This is counter-balanced by the random velocities originating from the combined influence of nucleon-nucleon collisions and Fermi motion. The measured enhancement is qualitatively reproduced by calculations which solve the Boltzmann-Uehling-Uhlenbeck equations.[9-11]

3. CIRCULAR POLARIZATION MEASUREMENTS OF Y-RAYS IN COINCIDENCE WITH CHARGED PARTICLES.

Since the collective motion in the nuclear mean field is damped by individual nucleon-nucleon collisions, the relative importance of positive and negative emission angles is sensitive to the sign of the mean field and to the interplay between mean field dynamics and two-body nucleon-nucleon dissipation.[2,11] We have addressed this issue experimentally by determining the sign of the average emission angle of non-equilibrium light particles from the circular polarization of associated Y-rays emitted by the residual nucleus for ^{14}N induced reactions on ^{154}Sm at E/A = 35 MeV.

3.1. Experiment

Metallic self-supporting ^{154}Sm targets of 4 and 11 mg/cm² areal density were bombarded with ^{14}N ions of 490 MeV energy. Light particles (Z ≤ 2) were detected with four ΔE-E telescopes arranged in a doubly symmetric geometry[12] at polar angles of θ=30° and θ=60° and azimuthal angles of φ=0° and 180° with respect to the beam axis. The telescopes consisted of 400 μm thick surface barrier detectors and 10 cm thick NaI detectors and subtended solid angles of ΔΩ(30°)=44 msr and ΔΩ(60°)=53 msr. To detect heavier charged particles (3 ≤ Z ≤ 15), the thinner target of 4 mg/cm² was used and two telescopes, each consisting of three Si detectors with thickness

of 30μmm, 50μmm and 2000μmm, were placed at θ=35°. The circular polarization of coincident Y-rays was measured with two forward scattering polarimeters[12] positioned at θ=90°, φ=90° and θ=90°, φ=270°. The polarimeters had in-beam analysing powers of 0.95±0.1% at the bombarding energies of E/A=35 MeV. The measured polarizations of light particles detected at θ=30° and θ=60° are very similar. For simplicity, only light particle data at θ=30° and heavy fragment data at θ=35° are shown here. Detailed description of the light particle data at θ=60° and the data at both angles for E/A=20 MeV can be found in ref. 11.

3.2. Experimental Results

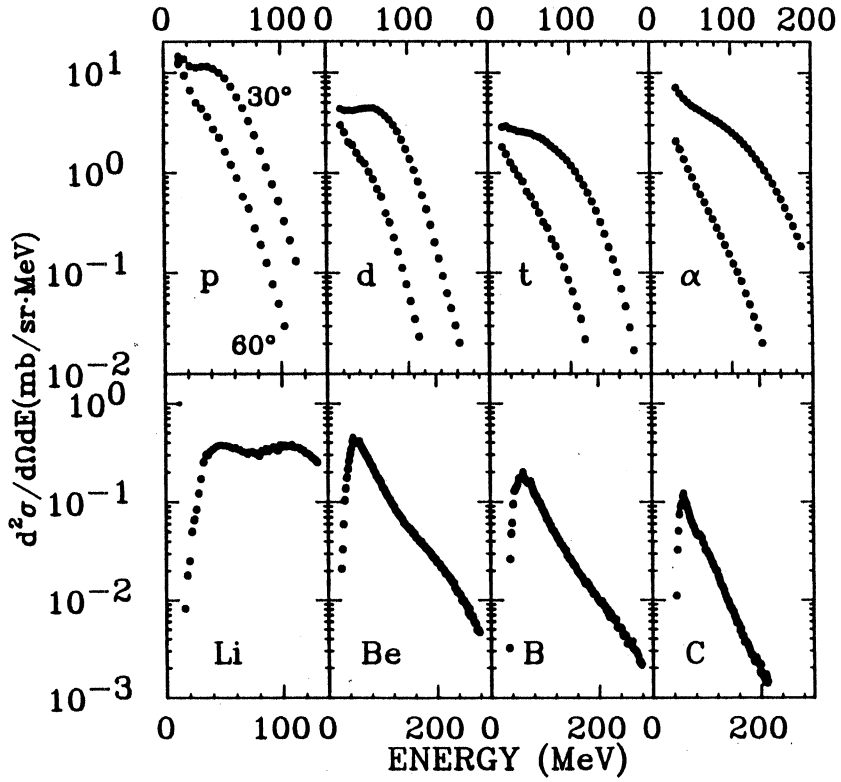

FIGURE 3
Inclusive energy spectra for p, d, t, and α detected at θ=30° and 60° (upper part) and for Li, Be, B and C detected at θ=35° (lower part) for ^{14}N induced reaction on ^{154}Sm at E/A = 35 MeV

The measured energy spectra for p, d, t, α, Li, Be, B and C are shown in Fig. 3. For the light particles, p, d, t, and α, data were taken at two polar angles, 30° and 60°. The cross sections are forward peaked and the energy spectra exhibit nearly exponential slopes in agreement with the trends established previously for nonequilibrium charged particle emission.[13-15] At 30°, the light particle spectra are dominated by non-equilibrium processes.[5,13-15]

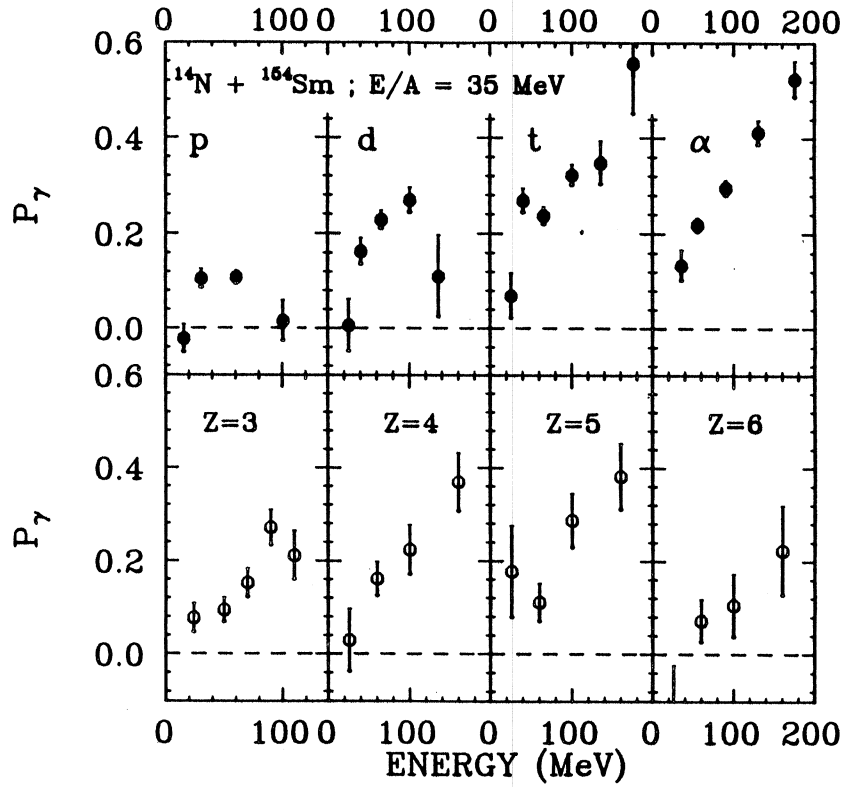

FIGURE 4
Circular Y-ray polarizations plotted as a function of particle energies for p, d, t, and α detected at θ=30° (upper part) and for Li, Be, B and C detected at θ=35° (lower part) for ^{14}N induced reaction on ^{154}Sm at E/A = 35 MeV

For the heavier fragments, inclusive data for fragments ($3 \leq Z \leq 15$) were taken only at 35°. However, more complete angular distributions of intermediate fragments have been measured for similar systems, such as ^{12}C + ^{197}Au at E/A = 30 MeV,[16] ^{14}N + Ag at E/A = 35 MeV[17,18] and ^{32}S + Ag at E/A = 22.5 MeV.[6] Analysis of the

inclusive data with a simple moving source parametrization suggests that the heavier intermediate mass fragments originate mainly from the colder and slower, hence, larger sources.[16] Another approach involves fitting the intermediate mass fragment energy spectra with a single parametrization which includes both a compound nucleus and a nonequilibrium source, each emitting isotropically with a Maxwellian energy distribution in its respective rest frame. The latter analysis suggests that the relative contribution from the fusion-like source increases with increasing fragment mass, becoming the dominant contribution for $Z \geq 8$.[6,17]

In our sign convention,[12] the quantization axis $\hat{n}$ is defined by: $\hat{n}=\vec{k}_i \times \vec{k}_f / |\vec{k}_i \times \vec{k}_f|$ where $\vec{k}_i$ and $\vec{k}_f$ are the momentum vectors of the beam and the detected particle respectively; positive circular Y-ray polarizations correspond to negative deflection angles and vice versa. The charged particle Y-ray polarizations are shown in Fig. 4. Positive polarizations are observed for all particles. Our experiment clearly establishes the preferential emission of non-equilibrium particles to negative emission angles, consistent with an attractive nuclear mean field and with measurements at lower energies.[19,20]

The magnitude of the measured polarization increases with increasing energy and mass of the coincident light particles up to alpha particles. This trend is more clearly shown when the polarizations are plotted as a function of the energy per nucleon of the detected light particles (p, d, t, α) as in Fig. 5. The lines are drawn to guide the eyes. The linear dependence of the polarization on particle mass at fixed velocity is similar to that expected from a coalescence mechanism for light particle production.[21]

For charged particles with $Z \geq 2$, no significant trend of polarization with particle mass can be discerned. The trend of increasing polarization with increasing particle velocity is well established with the heavier particles, following closely the trend previously established for the alpha particles, see Fig. 6. (Here, the solid and dashed lines are the same as those for the proton and alpha particle data which were drawn to guide the eye in Fig. 5.) The general dependence of the polarization on particle velocity for $Z \geq 2$ is suggestive of a common production mechanism. The magnitude (<50%) of the measured circular polarization is significantly smaller than the maximum polarization (~ 65%) one would calculate

from the estimated dealignment of the angular momentum of the residual system.[11] Such small polarizations imply that particles are scattered to both positive and negative angles.

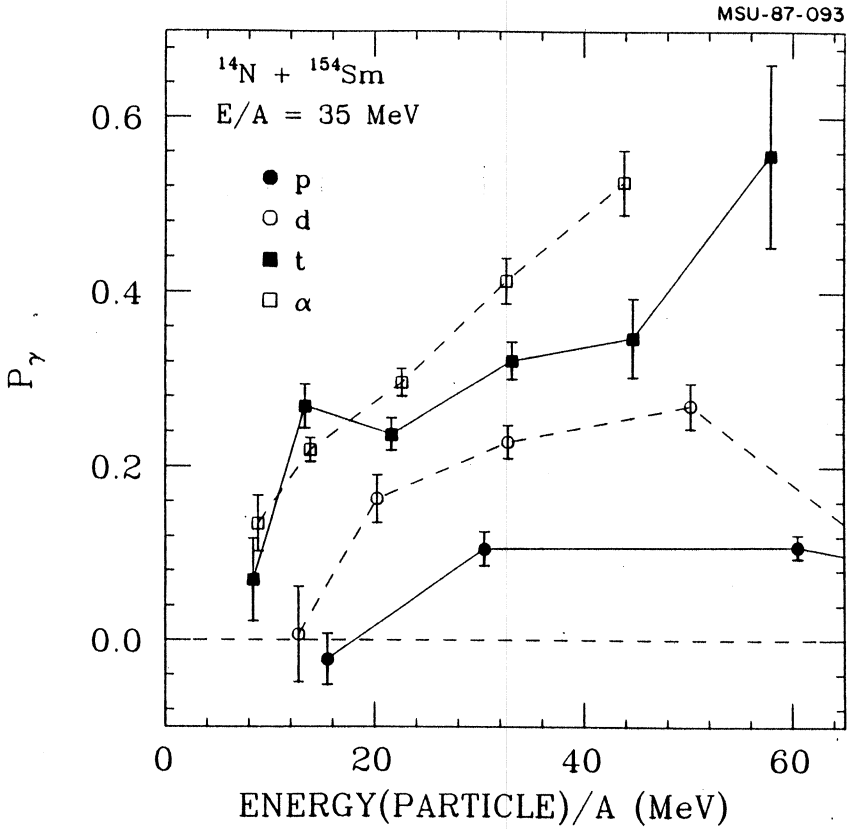

FIGURE 5
Circular γ-ray polarizations plotted as a function of particle energies per nucleon for p, d, t and α. The solid and dashed lines are drawn to guide the eye.

Small polarizations measured for low energy fragments suggest that low velocity fragments are emitted at the later more equilibrated stage of the reaction. This interpretation is consistent with the analysis of intermediate mass fragment inclusive data using moving sources parametrizations[6,16-18] discussed earlier. If a similar system, ^{14}N + Ag at E/A = 35 MeV,[17,18] and the procedure outlined in ref. 6 are used to estimate and subtract out

contributions from the compound nucleus emission for all the fragments, polarizations of the remaining non-equilibrium component increase to about 30%. For particle energy greater than 10 MeV per nucleon, contribution from the compound nucleus emission is negligible and the observed trend of increasing polarization with increasing particle velocity shown in Fig. 6 remains unchanged.

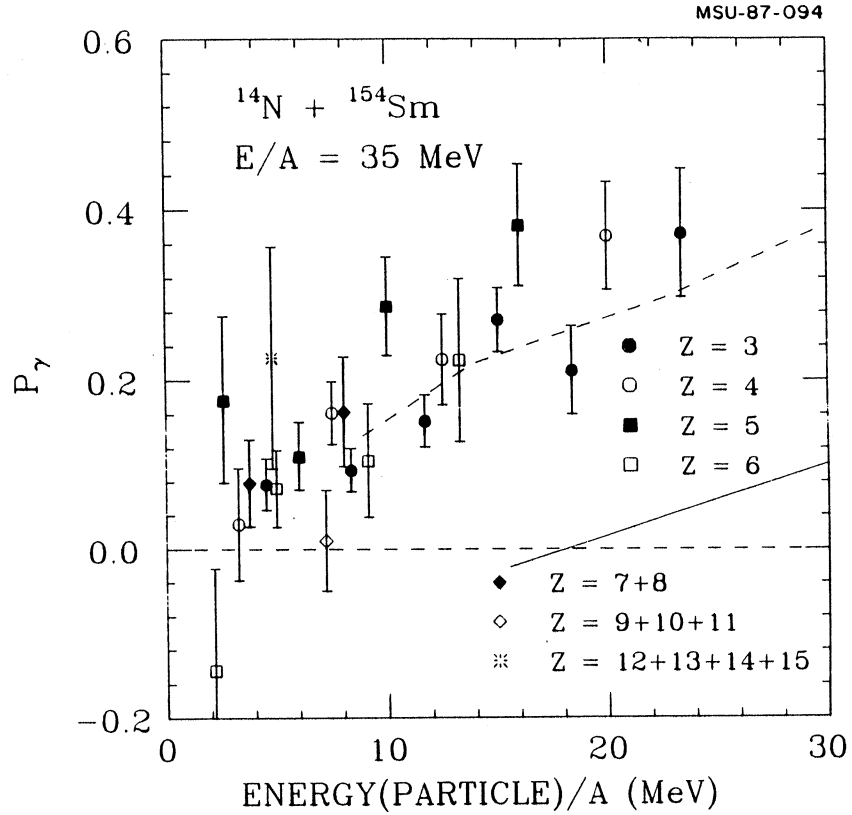

FIGURE 6
Circular γ-ray polarizations plotted as a function of particle energies per nucleon for Z=3 to Z=15 fragments. The solid and dashed lines are trends established by the proton and alpha data.

3.3. Numerical Solution of the Boltzmann-Uehling-Uhlenbeck equation

We have performed numerical calculations with the Boltzmann-Uehling-Uhlenbeck (BUU) equation[9-10] for ^{14}N+^{154}Sm collisions at

E/A=35 MeV with impact parameters between b=1 to 10 fm.[11] A Skyrme-type interaction with a compressibility coefficient of K=200 MeV and an isotropic nucleon-nucleon cross section of σ_{NN}=41 mb were used. The calculations predict the preferential emission of nucleons to negative angles, in qualitative agreement with the experimental observations. To allow a more quantitative comparison with the data, we have calculated the circular polarization predicted by the BUU model. The angular momentum, $\vec{J}(b)$, of the residual nucleus (assumed to correspond to nucleons within a radius of 7.5 fm at the collision time of 200 fm/c) was determined for each impact parameter. For simplicity, the residual nucleus was assumed to decay via stretched E2 transitions, corresponding to a Y-ray multiplicity of $M_\gamma = J(b)/2$. Integrating over the geometry of the polarimeters[12] Ω_γ, and averaging over impact parameters b, gives for the predicted polarization:

$$\langle P_\gamma(\theta)\rangle = \frac{2\pi \sum_b b\, M_J(b) \int dE \int d\phi\, \sigma_N(\theta,\phi,E) \int d\Omega_\gamma P(\beta) Y(\beta)}{2\pi \sum_b b\, M_J(b) \int dE \int d\phi\, \sigma_N(\theta,\phi,E) \int d\Omega_\gamma Y(\beta)} \qquad (3)$$

Here $Y(\beta)=1-\cos^4\beta$ and $P(\beta)=2\cos\beta/(1+\cos^2\beta)$ are the angular distribution of the Y-ray yield and circular Y-ray polarization, respectively, and $\cos(\beta) = \vec{k}_\gamma \cdot \vec{J}/(k_\gamma J)$; $\vec{k}_\gamma$ is the momentum vector of the emitted photon and $\sigma_N(\theta,\phi,E)$ is the nucleon differential cross section. The polarization is integrated over the azimuthal angles of the emitted nucleons and over energies greater than 30 MeV. At 30° and 60°, the predicted polarizations are 0.15±0.03 and 0.20±.03, respectively. The values have been reduced by 20% by taking into account non-stretched transitions.[22,23] The calculated polarizations are larger than the experimentally observed proton polarizations of 0.1. However, the present calculations do not include emission of composite particles which have larger measured polarizations. One may assess the effects of complex particle emission by evaluating an "effective nucleon polarization" according to the definition:

$$P_{eff}(\theta) = \frac{\sum_i \sum_j A_i \sigma_i(\theta,E_j) P_i(\theta,E_j)}{\sum_i \sum_j A_i \sigma_i(\theta,E_j)} \qquad (4)$$

where A_i, $P_i(\theta,E_j)$ and $\sigma_i(\theta,E_j)$ denote mass, experimentally measured polarization and cross section for particle i and i=p,d,t,α. For particle energies E/A≥30 MeV, the effective polarizations are

$P_{eff}(30°) = 0.24\pm0.04$ and $P_{eff}(60°) = 0.17\pm0.04$. Considering the experimental uncertainties of the absolute calibrations of the analysing power and the theoretical uncertainties in the relative weights for the composite particles, $P_{eff}(\theta)$ and the calculated polarizations $\langle P_\gamma(\theta)\rangle$ are in reasonable agreement.

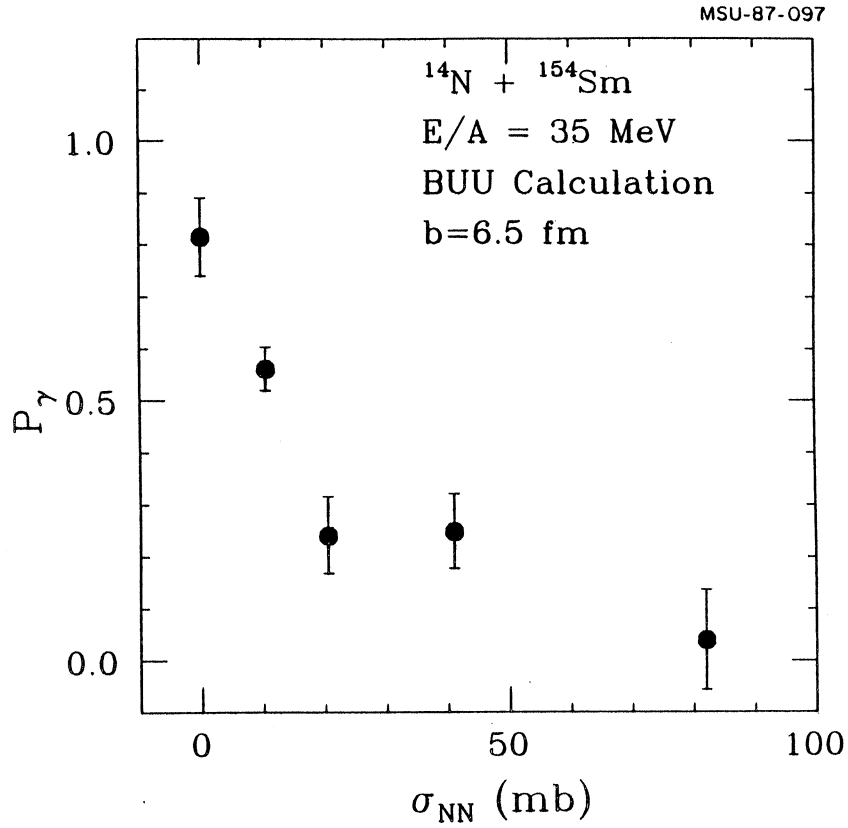

FIGURE 7
Predicted Y-ray circular polarization as a function of the nucleon-nucleon interaction cross-section.

In order to illustrate the dependence of the predicted polarizations on the nucleon-nucleon collision dynamics, we have varied the strength of the residual interaction. For simplicity, calculations were only performed for one impact parameter, b=6.5 fm. This impact parameter contributes the largest weight to the polarization integral of equation 3. Fig. 7 shows the dependence of the predicted polarization on the strength of the nucleon-nucleon

scattering cross section. The predicted polarization decreases monotonically with increasing values of σ_{NN}. For σ_{NN}= 41 mb, the polarization is reduced by over a factor of three below the value calculated with the mean field alone. Thus the magnitude of the impact parameter averaged polarizations calculated with equation 1 reflects the balance between deflection by the mean field and randomization of the particle velocities by nucleon-nucleon collisions.

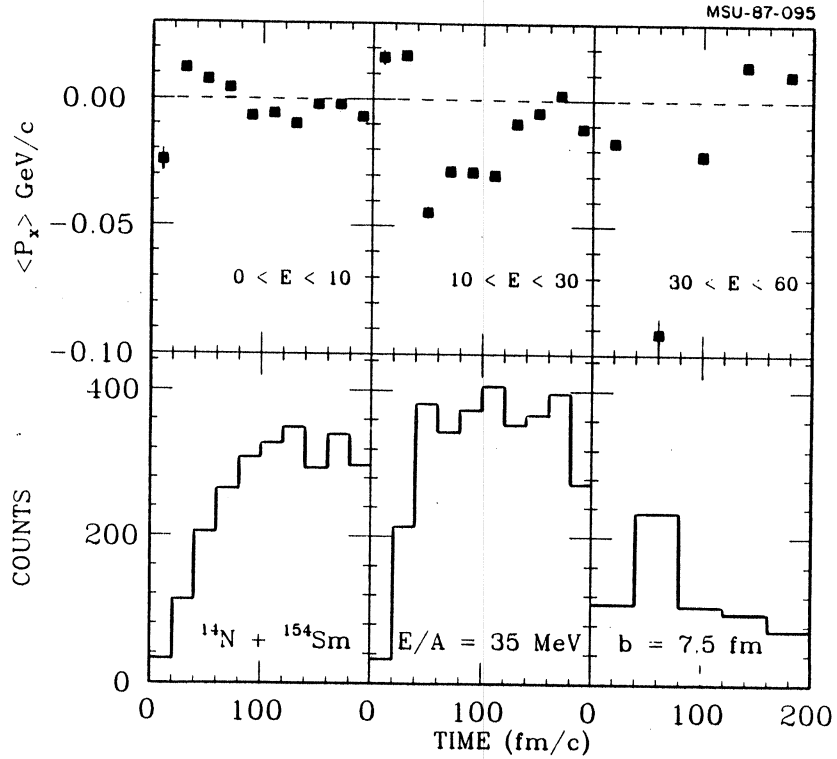

FIGURE 8
Number of nucleons emitted as a function of time (lower part). In the upper part, the corresponding mean transverse momenta for the nucleons emitted in the time interval is plotted. The left, center and right part of the figure correspond to energy gates of 0-10, 10-30 and 30-60 MeV respectively.

All charged particles are preferentially emitted to negative angles. By observing the sign of the averaged transverse momentum ($\langle P_x \rangle$) of the emitted nucleons, one can get an estimate of the

emission time of the detected particles. In our convention, the z-axis is designated to be parallel to the projectile linear momentum. The x-axis is chosen to lie in the reaction plane. For non-zero impact parameters, the projectile is displaced to positive values of x; positive $\langle P_x \rangle$ (negative $\langle P_x \rangle$) corresponds to emission to the same (opposite) side of the target as the initial impact.

The results of the BUU calculations performed at b=7.5 fm are shown in Fig. 8. The lower part of the figure shows the number of nucleons emitted at fixed time intervals. The top part of the figure shows the average transverse momentum for the nucleons emitted during those time intervals. Results are shown for three different energy ranges of the emitted particles. The left hand part of the figure corresponds to nucleons emitted with energy less than 10 MeV per nucleon, the center part corresponds to the energy interval between 10 to 30 MeV per nucleon and the right hand part corresponds to nucleons with energies between 30 and 60 MeV. The majority of the low energy particles are emitted on time scales greater than 150 fm/c. The transverse momenta of these nucleons are small, very close to 0. The calculations suggest that low velocity nucleons are emitted at the later stages of the emission with the measured polarization close to zero. Most nonequilibrium charged particles with energies between 10 to 30 MeV per nucleon are emitted with large negative transverse momentum during the time interval of approximately 50 to 150 fm/c. The highest energy nucleons ($\geq$ 30 MeV/A) are primarily emitted during a short time interval around 60 fm/c. However, there seems to be a constant background of nucleons emitted at later time. The average transverse momentum of the nucleons emitted outside the time window of 40 to 80 fm/c is close to zero and even becomes positive. This constant background of nucleons (random velocity components) emitted both to positive and negative scattering angles limits the value of the predicted circular polarization to values less than one even for the ideal case of perfect spin alignment.

The present formulation of the Boltzmann equation has the drawback that it does not treat fluctuations of the mean field and therefore cannot properly account for the emission of large complex fragments. Thus the trends displayed by complex particle polarization cannot be explained quantitatively. However, progress is being made to include complex particles into the Boltzmann equations. Several approaches are being discussed at this

conference.[24-26] Quantitative comparisons between model calculations and experimental data for fragment emission may be possible in the near future. Even with the present formulation, calculations using the BUU equations will provide insights concerning the dynamics of particle emission as well as the interplay between mean field dynamics and nucleon collisions at intermediate energies.

4. TRANSVERSE MOMENTUM DISTRIBUTIONS AS A FUNCTION OF BOMBARDING ENERGIES

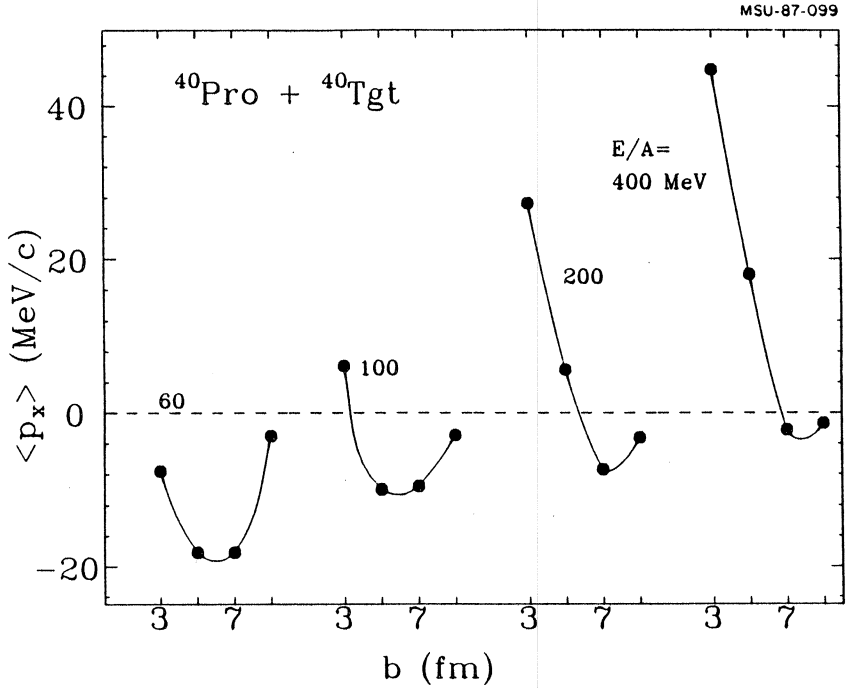

FIGURE 9
Mean transverse momenta calculated for mass 40 projectiles and mass 40 targets, impact parameters of 3, 5, 7 and 9 fm, and bombarding energies of E/A = 60, 100, 200 and 400 MeV.

To study how the average transverse momentum evolves as a function of bombarding energy, we have performed BUU calculations[2] between mass 40 projectiles and mass 40 targets for bombarding energies of E/A = 60, 100, 200, and 400 MeV and impact parameters of 3, 5, 7, and 9 fm. The results are shown in Fig. 9. At low energies, the majority of energetic nucleons are deflected by the attractive mean field and emerge with negative transverse momenta, consistent

with the polarization measurements discussed earlier. The mean transverse momentum increases monotonically with bombarding energy. This is particularly evident at smaller impact parameters where $\langle P_x \rangle$ changes sign and becomes positive for E/A > 100 MeV. A similar trend was reported in Ref 1. Positive momentum transfers are consistent with the interpretation of momentum distributions measured with the Plastic Ball at the Lawrence Berkeley Laboratory.[27] (Note however, the sign of the emission angles cannot be determined from the Plastic Ball data.) A similar dependence of the transverse momentum with impact parameters is reported[28] by Harris et al for the ^{197}Au + ^{197}Au reactions at E/A = 200 MeV at this conference. These positive transverse momenta arise from the scattering of nucleons by the repulsive nuclear mean field present during the high density stage of the collision and from the kinetic pressure caused by the incoherent nucleon-nucleon collisions represented by the collision term.

5. SUMMARY

In summary, nonequilibrium light particles produced in fusion-like reactions of ^{14}N + ^{197}Au at E/A = 30 MeV are preferentially emitted in the entrance-channel scattering plane. The measured azimuthal anisotropies increase significantly for heavier and more energetic particles. The observed in-plane enhancement suggests an ordered transverse motion in the reaction plane superimposed on the random statistical motion of the individual nucleons. Measurements of the circular polarizations of Y-rays in coincidence with charged particles indicate that non-equilibrium particles are predominantly emitted to negative emission angles. Negative emission angles are consistent with the deflection of non-equilibrium particles by an attractive nuclear mean field. Calculations with the Boltzmann-Uehling-Uhlenbeck equation predict preferential emission to negative angles. The BUU calculations suggest that collisions between individual nucleons reduce the polarizations significantly below what might be expected from pure mean field dynamics such as described by TDHF or Vlasov calculations. Non-equilibrium particles are emitted between 50 to 150 fm/c after the projectile and target reach the point of closest approach. By examining the average transverse momentum $\langle P_x \rangle$ as a function of bombarding energy, the scattering angle for the non-equilibrium particles is predicted to change sign as the bombarding energy E/A is increased above 100 MeV

due to the weakening of the attractive nuclear mean field and to the increased importance of nucleon-nucleon collisions at higher energies.

ACKNOWLEDGEMENT

The author wishes to thank Drs. W. Dünnweber, C.K. Gelbke, K. Kwiatkowski, W.G. Lynch, J. Pochodzalla, R.M. Ronningen, W. Trautmann, and V. Viola for valuable help during the experiments and enlightening discussion afterwards. The author would also like to thank Dr. J. Aichelin for installing his program at the NSCL computer and to thank Dr. G. Bertsch for helpful suggestions. This work has been supported by the National Science Foundation under Grant No. PHY-85-19653.

REFERENCES

1) J.J. Molitoris, D. Hahn and H. Stöcker, Nucl. Phys. A447, 13c (1985)
2) G.F. Bertsch, W.G. Lynch, and M.B. Tsang, Phys. Lett. (in press)
3) C. Gregoire, B. Remaud, F. Sebille, and L. Vinet, Phys. Lett 186B, 14 (1987).
4) M.B. Tsang, C.B. Chitwood, D.J. Fields, C.K. Gelbke, D.R. Klesch, W.G. Lynch, K. Kwiatkowski and V. E. Viola, Jr., Phys. Rev. Lett. 52, 1967 (1984)
5) M.B. Tsang, W.G. Lynch, C.B. Chitwood, D.J. Fields, D.R. Klesch, C.K. Gelbke, G.R. Young, T.C. Awes, R.L. Ferguson, F.E. Obenshain, F. Plasil and R.L. Robinson, Phys. Lett. 148B, 265 (1984)
6) D.J. Fields, W.G. Lynch, T.K. Nayak, M.B. Tsang, C.B. Chitwood, C.K. Gelbke, R. Morse, J. Wilczynski, T.C. Awes, R.L. Ferguson, F. Plasil, F.E. Obenshain and G.R. Young, Phys. Rev. C34, 536 (1986)
7) C.B. Chitwood, D.J. Fields, C.K. Gelbke, D.R. Klesch, W.G. Lynch, M.B. Tsang, T.C. Awes, R.L. Ferguson, F.E. Obenshain, F. Plasil, R.L. Robinson, and G.R. Young, Phys. Rev. C34 858 (1986).
8) W.A. Friedman, Proceedings of the Symposium on Central Collisions and Fragmentation Processes, National Meeting of the ACS, Denver, Co, April 5-10, 1987. Nucl. Phys. (in press)
9) J. Aichelin and G. Bertsch, Phys. Rev. C31, 1730 (1985).
10) J. Aichelin, Phys. Rev. C33 537 (1986)
11) M.B. Tsang, R.M. Ronningen, G. Bertsch, Z. Chen, C.B. Chitwood, D.J. Fields, C.K. Gelbke, W.G. Lynch, T. Nayak, J. Pochodzalla, T. Shea, and W. Trautmann, Phys. Rev. Lett. 57, 59 (1986)
12) W. Trautmann, C. Lauterbach, J. de Boer, W. Dünnweber, G. Graw, W. Hamann, W. Hering and H. Puchta, Nucl. Instr. and Meth. 184, 449 (1981)
13) T.C. Awes, G. Poggi, C.K. Gelbke, B.B. Back, B.G. Glagola, H. Breuer and V.E. Viola, Jr., Phys. Rev. C24, 89 (1981)

14) T.C. Awes, S. Saini, G. Poggi, C.K. Gelbke, D. Cha, R. Legrain, and G.D. Westfall, Phys. Rev. C25, 2361 (1982)
15) G.D. Westfall, B.V. Jacak, N. Anantaraman, M.V. Curtin, G.M. Crawley, C.K. Gelbke, B. Hasselquist, W.G. Lynch, D.K. Scott, B.M. Tsang, M.J. Murphy, T.J.M. Symons, R. Legrain and T.J. Majors., Phys. Lett. 116B, 118 (1982)
16) D.J. Fields, W.G. Lynch, C.B. Chitwood, C.K. Gelbke, M.B. Tsang, H. Utsunomiya and J. Aichelin, Phys. Rev. C30, 1912 (1984)
17) T. Nayak, private communications
18) M. Curtin, PhD thesis, Michigan State University, (1985)
19) W. Trautmann, Ole Hansen, H. Tricoire, W. Hering, R. Ritzka and W. Trombik, Phys. Rev. Lett. 53, 1630 (1984)
20) T. Fukuda, M. Ishijara, K. Iski, T. Shimoda, K. Ogura, S. Shimoura and H. Ogata, 6th International Symposium on Polarization Phenomena in Nuclear Physics. Osaka (Japan) 26-30 Aug, 1985 Pg. 116
21) T.C. Awes, C.K. Gelbke, G. Poggi, B.B. Back, B. Glagola, H. Breuer, V.E. Viola, Jr., and T.J.M. Symons, Phys. Rev. Lett. 45, 513 (1980)
22) W. Trautmann, W. Dünnweber, W. Hering, C. Lauterbach, H. Puchta, R. Ritzka and W. Trombik, Nucl. Phys. A422, 418 (1984).
23) D.G. Sarantites, L. Westerberg, M.L. Halbert, R.A. Dayras and H.C. Hensley, J.H. Barker, Phys. Rev. C18, 774 (1978)
24) C. Gregoire, Proceedings of the Symposium on Central Collisions and Fragmentation Processes, National Meeting of the ACS, Denver, Co, April 5-10, 1987. Nucl. Phys. (in press)
25) S. Das Gupta, Proceedings of the Symposium on Central Collisions and Fragmentation Processes, National Meeting of the ACS, Denver, Co, April 5-10, 1987. Nucl. Phys. (in press)
26) D. Boal, Proceedings of the Symposium on Central Collisions and Fragmentation Processes, National Meeting of the ACS, Denver, Co, April 5-10, 1987. Nucl. Phys. (in press)
27) H.A. Gustafasson, H.H. Gutbrod, B. Kolb, H. Lohner, B. Ludewigt, A.M. Poskanzer, T. Renner, H. Riedesel, H.G. Ritter, A. Warwick, F. Weik and H. Wieman, Phys. Rev. Lett. 52, 1590 (1984)
28) J. Harris, Proceedings of the Symposium on Central Collisions and Fragmentation Processes, National Meeting of the ACS, Denver, Co, April 5-10, 1987. Nucl. Phys. (in press)